Resolution of the Absorbance and CD Spectra and Formation Constants of the Complexes between Human Serum Albumin and Methyl Orange**

R. Ambrosetti, R. Bianchini,* S. Fisichella, M. Fichera, and M. Zandomeneghi

Abstract: Difference absorbance and circular dichroism techniques show that two complexes are formed between human serum albumin (HSA) and Methyl Orange (MO). The stoichiometries of the two HSA–MO complexes (1:1 (C_1) and 1:2 (C_2)), their association constants ($K_{1,1} = 2.32\ (0.18) \times 10^5\ M^{-1}$ and $K_{1,2} = 1.12\ (0.15) \times 10^{11}\ M^{-2}$), and both absorbance and dichroic spectra have been determined by a computational approach. Nearly 900 experimental points, consisting of absorbance and CD measurements registered in the 340–550 nm interval and over a wide range of concentrations of protein and ligand, have been included in a unique fitting procedure. The Scatchard plot indicates the existence of a unique binding site which can accommodate up to two molecules of MO in a positive cooperative process. Calculation of the CD spectrum for the C_2 complex according to the DeVoe method reproduces the fitted dichroic spectrum for the same complex. The shapes of the fitted absorbance and dichroic spectra, as well as the influence of concentrated NaCl or ethylene glycol on the absorbances of both free MO and HSA–MO mixtures are consistent with the presence of dominant electrostatic interactions in C_1. The C_2 complex can be envisaged as a unique chromophore, consisting of two MO units associated in a stacking process into the same binding site of HSA, leading to a well-defined chirality. The general validity of this multitechnique, multiwavelength approach in the investigation of protein–ligand complexes is discussed.

Keywords
azo dyes · circular dichroism · data fitting · formation constants · protein complexation

Introduction

The exceptional ability of serum albumins to reversibly bind organic molecules and ions has been well known for a long time.[1] This unique property enables albumins to fulfil a fundamental biological role as a universal carrier and reservoir in blood plasma, tissues, and secretions throughout the mammalian body.[2] Much effort has therefore been devoted to the thermodynamic and spectroscopic characterization of the complexes of albumins with a number of natural and synthetic ligands.[3] Investigation into the stabilities, stoichiometries, and other physicochemical aspects of these species can be included under the general topic of complexation of small molecules by macromolecules.[4]

Among the experimental techniques available for this purpose, spectrophotometric (UV/Vis, CD, fluorescence, etc.) studies have been most frequently undertaken, and a large number of data-handling methodologies, all requiring more or less restrictive starting hypotheses, have been utilized to manage the resulting experimental data.

In the present paper an investigation into the complexation of the human serum albumin (HSA) and Methyl Orange (MO, sodium 4-dimethylaminoazobenzene-4-sulfonate) in buffer (pH = 7.0) is presented. Many extensive studies of the interactions between dyes and polymers, both synthetic and biological, have been carried out.[5] Synthetic dyes are an effective class of compound for the cheap and efficient detection and purification of proteins.[6] The best example of this is affinity chromatography, in which the selective adsorption of a protein on a ligand immobilized on the stationary phase can be employed as a powerful method to separate the protein from a multicomponent mixture, recover the pure material, and regenerate the solid matrix.[7] Moreover, many synthetic dyes are increasingly being used as mimics of molecules endowed with high biological activity and as probes for studying specific interactions with proteins.[8] The azo dye Methyl Orange is one such dye, which has often been used as a probe to investigate the interactions of albumins, and other macromolecules, with organic anions.[9] The protein–dye interaction is usually accompanied by spectral changes not associated with the acid–base indicator properties of MO,[10] but depending instead on the protein/dye concentration ratio, as we will show later.

Here we report on the formation of two stable complexes between HSA and MO with 1:1 and 1:2 stoichiometries. Their association constants, molar absorptivities, and ellipticities in the 340–540 nm interval have been derived by a recently proposed computational approach, and the nature of the dye–protein binding has been investigated in both complexes.

[*] Prof. Dr. R. Bianchini, Prof. Dr. S. Fisichella, Dr. M. Fichera
Dipartimento di Scienze Chimiche
V. le A. Doria 6, Catania 95125 (Italy)
Telefax: Int. code +(95)580-138; (50)43321
Res. Dir. Dr. R. Ambrosetti
Istituto di Chimica Quantistica ed Energetica Molecolare, CNR
via Risorgimento 35, Pisa 56126 (Italy)
Prof. Dr. M. Zandomeneghi
Dipartimento di Chimica e Chimica Industriale, Università di Pisa
via Risorgimento 35, Pisa 56126 (Italy)

[**] A preliminary communication has been presented at the 12th Conference on Physical Organic Chemistry (IUPAC), Padua (Italy), **1994**, Abstracts, p. 82.

  0947-6539/96/0202-0149 $ 10.00+.25/0

Results

Spectrophotometric Measurements: A set of spectrophotometric investigations, consisting of difference UV/Vis absorbance spectra[11] registered in the 300–700 nm interval, was carried out. The protein and dye concentrations examined ranged from 1×10^{-6} to 1.53×10^{-4} M and from 1.3×10^{-6} to 5.4×10^{-5} M, respectively, and the [HSA]/[MO] ratio from 9.72 to 0.06. In Figure 1 (solid lines) the curves of type 1 are the difference UV/Vis spectra recorded at a constant MO concentration of 1.57×10^{-5} M and variable concentrations of HSA ($0.15-15.3\times10^{-5}$ M); those of type 2 are taken from mixtures containing a constant HSA concentration of 1.0×10^{-5} M and variable concentrations of MO ($0.13-5.44\times10^{-5}$ M). Higher concentrations of the species present in excess could not be attained. In fact, because of its molecular weight (67000), an HSA concentration of 1.6×10^{-4} M corresponds to a 1% (w/w) albumin solution. Higher concentrations of HSA could result in the formation of dimers or higher aggregates. Because of the large molar absorptivities of Methyl Orange in the examined spectrophotometric range, dye concentrations greater than 5×10^{-5} M would give nearly opaque solutions, and the registered difference absorbances would be unreliable.

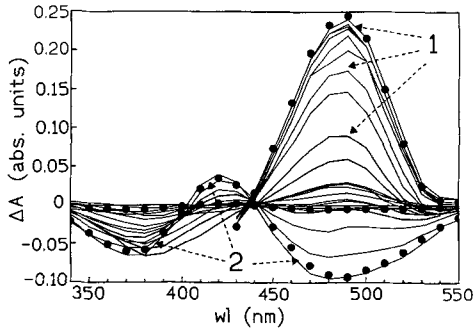

Fig. 1. Difference absorbance spectra of solutions of MO and HSA in 0.1 M phosphate buffer (pH = 7.0, 1 cm path). Curves of type 1: $[MO]_t = 1.57\times10^{-5}$ M, $[HSA]_t = 0.102-15.26\times10^{-5}$ M; curves of type 2: $[HSA]_t = 1\times10^{-5}$ M, $[MO]_t = 0.13-5.44\times10^{-5}$ M. The filled circles represent the fitted curves corresponding to the highest, the lowest, and an intermediate [HSA]/[MO] ratio.

Inspection of Figure 1 reveals that different species are formed depending on the [HSA]/[MO] ratio. In the presence of excess protein (curves 1) a negative peak with a minimum at 370–380 nm is obtained, together with a larger, positive absorbance centered at 490 nm. Also, an apparent saturation of the dye at the highest albumin concentrations reached seems to occur. With a large excess of MO at a constant concentration of HSA (curves 2), two negative difference absorbance bands, in the 350–420 and 450–550 nm ranges, together with a small positive peak at 420 nm, are exhibited. An isosbestic point occurs at around 440 nm in both sets of experiments, indicative, as we will show later (see Fig. 3), of an equilibrium between complexes and free MO.

The fact that at least two different complexes are formed depending on the ratio between the concentrations of the starting materials is also indicated by the CD spectra, reported in Figure 2 (solid lines). Here, the appearance of CD spectra must be attributed to the bound dye, since the HSA chromophores do not display CD activity in the 350–550 nm interval. At high [HSA]/[MO] ratios two negative peaks are recorded around 400 and 490 nm (curves 1), while at ratios of less than one drastic changes occur; the resulting spectra exhibit a negative band

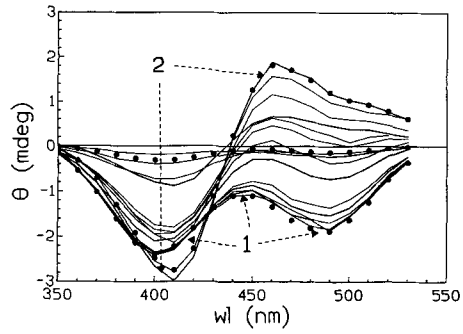

Fig. 2. Dichroic spectra of solutions MO and HSA in 0.1 M phosphate buffer (pH = 7.0, 0.5 cm path). Curves of type 1: $[MO]_t = 1.49\times10^{-5}$ M, $[HSA]_t = 0.103-15.02\times10^{-5}$ M; curves of type 2: $[HSA]_t = 0.9\times10^{-5}$ M, $[MO]_t = 0.12-5.96\times10^{-5}$ M. The filled circles represent fitted curves corresponding to the highest, the lowest, and an intermediate [HSA]/[MO] ratio.

centered at 410 nm and a positive maximum at 460 nm (curves 2). An apparent saturation of the dye seems to take place at high [HSA], as was implied from the UV/Vis difference absorptions of Figure 1. Correspondingly, a total complexation of the albumin was apparent in solutions with higher concentrations of MO. Moreover, an isodichroic point appears at 430 nm in the set of spectra at constant $[MO]_{total}$ ($[MO]_t$).

The UV/Vis absorbance (539) and dichroic (340) data consisted of 879 experimental points, collected in the 340–550 nm range; the values at 22 discrete wavelengths (340, 350, 360 ... 540, 550 nm) were taken into account. The spectroscopic data outside this wavelength range were excluded, because of the protein contribution to the overall difference absorbance (300–340 nm) and because of the low signal-to-noise ratio (CD, 560–600 nm).

Computational Approach: Although most literature data on the association of biological macromolecules are obtained from plots of bound fraction vs. bound concentration of the Scatchard type,[12] we adopt a conceptually simpler and straightforward method based on elementary stoichiometry.[13] This approach allows us to fit data, collected by different experimental techniques, to a model describing the formation of each possible A_mB_n complex. Since the experimental data are spectrophotometric quantities that are proportional to concentration, we introduce proportionality constants (differential extinction coefficients for difference absorbance and molar ellipticities for circular dichroism) in order to compare computed and experimental quantities. Comparison was achieved by a nonlinear least-squares (NLLSQ) method.[14]

In this procedure, the "experimental data" consist of a set of five measurements taken on each chemical sample, namely, the total concentrations ($[A]_t$ and $[B]_t$), the wavelength, the optical pathlength, and the spectroscopic quantity (absorbance, ellipticity, etc.). Fitting parameters are the formation constants of all complexes involved, and the molar absorptivities (and molar ellipticities in the present application) of each complex, at each wavelength.

We can obtain the equilibrium concentrations of all complexes by means of the equations based on conservation of mass for both species A and B [Eqs. (1) and (2)]. Substitution of Equation (3) into (1) and (2) gives two new equations, containing

$$[A]_t = [A] + \sum_{m,n}(m[A_mB_n]) \quad (1)$$

$$[B]_t = [B] + \sum_{m,n}(n[A_mB_n]) \quad (2)$$

$$[A_mB_n] = K_{m,n}[A]^m[B]^n \quad (3)$$

0947-6539/96/0202-0150 $ 10.00+.25/0 Chem. Eur. J. 1996, 2, No. 2

equations, containing only [A] and [B] as unknowns and the expression for the concentration of complexes as a function of [A] and [B] [Eq. (3)]. The numerical solution of the above system is accomplished by following a Newton–Raphson procedure.[15]

Although the fitting program can be used to treat many different stoichiometries, only the A_mB_n complexes having $m = 1$ and $n = 1$ and 2 have been included: A stands for HSA and B for MO. The simplest hypothesis for the stoichiometries of the complexes C_1 and C_2, suggested by the data displayed in Figures 1 and 2, is 1:1 for C_1 and 1:2 for C_2; the equilibria in which they are formed are shown in Equations (4) and (5). The two

$$HSA + MO \rightleftharpoons C_1 \quad (4)$$

$$C_1 + MO \rightleftharpoons C_2 \quad (5)$$

association constants K_1 and K_2 for the formation of C_1 and C_2 are defined by Equations (6) and (7). It is worth noting that,

$$K_1 = [C_1]/[HSA]_{free}[MO]_{free} \quad (6)$$

$$K_2 = [C_2]/[C_1][MO]_{free} \quad (7)$$

while K_1 is coincident with the $K_{1,1}$ obtained through the fitting procedure, K_2 is given by Equation (8).

$$K_2 = K_{1,2}/K_{1,1} \quad (8)$$

The fitting procedure requires preliminary assumptions for the parameters $K_{1,1}$ and $K_{1,2}$ and, moreover, for all molar absorptivities and ellipticities at all wavelengths in the examined range. To start with reasonable values for these parameters, we looked at the extreme curves, both absorbance and dichroic, reported in Figures 1 and 2, from which limiting absorbance and CD spectra could be evaluated. Moreover, a tentative value for $K_{1,1} = 1/([HSA]_t - [C_1]) \approx 1 \times 10^5\,M^{-1}$ was estimated, assuming that a 50% complexation of the dye could occur at $[HSA]_t \approx 2.5 \times 10^{-5}\,M$ (Fig. 1, curves 1). We also used a value for $K_{1,2}$ of $10^{10}\,M^{-2}$ as starting parameter, obtained by a similar approach.

We tried first to separately fit absorbance and dichroic data. In both attempts we obtained a satisfactory fit, as shown by the variance of the fittings reported in Table 1. But the computed values of the $K_{1,1}$ and $K_{1,2}$ association constants were quite different in the two runs: $K_{1,1} = 2.62 \times 10^5\,M^{-1}$ and $K_{1,2} = 4.27 \times 10^{10}\,M^{-2}$ were obtained from the UV/Vis data (run 1), while the corresponding best-fit values from dichroic data (run 2) were $K_{1,1} = 1.03 \times 10^5\,M^{-1}$ and $K_{1,2} = 1.17 \times 10^{11}\,M^{-2}$. Relative standard deviation was 15% in both runs for $K_{1,2}$, and 7% in run 1 and 15% in run 2 for $K_{1,1}$. The correlation between the two parameters was high and positive in both cases. Finally, a much higher value for the r.m.s. of the residuals of spectra was computed in run 2. This finding reflects the higher values in the measured CD data (about 10 times greater than typical difference absorbance data) rather than the quality of the fit.

A fitting including both absorbance and dichroic measurements was then carried out (run 3). The inclusion of spectroscopic data of both techniques (879 experimental points, see Experimental Procedure) results in an improvement of the fitting: the correlation coefficient becomes lower (0.985), and the relative standard deviations of $K_{1,1}$ and $K_{1,2}$ are 14 and 13%, respectively. It is evident that the computed values for both constants closely resemble those obtained in run 2. This result stems from the larger CD data set, which almost exclusively control the residuals.

We then attempted a final fit (run 4) on the complete set, this time having multiplied the absorbance data by 10. This is equivalent to giving roughly equal weight both to absorbance and CD data. An excellent convergence was obtained to $K_{1,1}$ and $K_{1,2}$ values of 2.32×10^5 (0.18) M^{-1} and 1.123×10^{11} (0.15) M^{-2}, respectively. It is worth stressing that this overall fitting furnishes well-defined $K_{1,1}$ and $K_{1,2}$ values, as shown by the standard deviations relative to $K_{1,1}$ and $K_{1,2}$ (8 and 13% of the reference parameter), which are significantly lower than in the other reported attempts, even though the correlation between them remained almost unchanged ($r = 0.983$). Finally, the fitted (filled circles) and experimental (solid lines) absorbance and dichroic curves compared in Figures 1 and 2 exhibit considerable agreement. The set of parameters obtained from run 4 fits the data of run 1 with only a slight increase in the r.m.s. deviation (to 0.008 abs. units). This is not surprising, when one considers the very high correlation of $K_{1,1}$ and $K_{1,2}$ for run 1, which implies some degree of ambiguity in the best fit parameters.

Besides the $K_{1,1}$ and $K_{1,2}$ values, the fitting results provide the molar difference absorptivities and the molar ellipticities of both C_1 and C_2 complexes. In Table 2 we report these spectral data; the spectra of the complexes are shown as Figures 3 (absorbance, curves 1 and 2) and 4 (CD, solid lines) and will be discussed later.

Having obtained values for $K_{1,1}$ and $K_{1,2}$, we were able to calculate the equilibrium concentrations of all species (HSA, MO, C_1, and C_2) for each set of HSA and MO total concentrations. These values are reported in Figure 5, where [MO] $= 1.57 \times 10^{-5}$ and [HSA] $= 0.1 - 15.3 \times 10^{-4}\,M$, and in Figure 6, where total [HSA] $= 1.0 \times 10^{-5}\,M$ and [MO] $= 0.13 - 5.44 \times 10^{-5}\,M$. Looking at these curves, we can conclude that both C_1 and C_2 complexes are present at all examined experimental concentrations of HSA and MO. Thus it can be inferred that it is not possible to isolate either C_1 or C_2 at the highest experimentally attainable reagent concentrations.

Finally, looking at equilibria (4) and (5) and applying Equations (6)–(8), we can calculate that $K_1 = 2.32 \times 10^5$ (0.18) M^{-1} and $K_2 = 4.83 \times 10^5$ (0.27) M^{-1}.

Traditional Data-Handling Methodologies: The results obtained by the computational approach described above could in prin-

Table 1. Association constants for the formation of C_1 ($K_{1,1}$, 1:1 stoichiometry) and C_2 ($K_{1,2}$, 1:2 stoichiometry) complexes between HSA and MO obtained through the fitting procedure.

Run	Technique	Data points	$K_{1,1}/\times 10^5\,M^{-1}$	$K_{1,2}/\times 10^{10}\,M^{-2}$	r.m.s. [a]	r [b]
1	UV/Vis	549	2.62 (0.19)	4.27 (0.62)	0.007	0.994
2	CD	340	1.03 (0.15)	11.7 (1.8)	0.088	0.988
3	UV/Vis +CD	879	1.05 (0.15)	11.2 (1.5)	0.076	0.985
4	UV/Vis +CD	879	2.32 (0.18)	11.2 (1.5)	0.087	0.983

[a] Root mean square deviation of calculated and experimental spectra, reported in absorbance or/and ellipticity units. [b] Correlation coefficient between the two fitting parameters ($K_{1,1}$ and $K_{1,2}$).

Table 2. Computed molar difference absorptivities and ellipticities of C_1 and C_2 complexes.

λ/nm	C_1 (diff. abs.)/ $M^{-1}cm^{-1}$	C_2 (diff. abs.)/ $M^{-1}cm^{-1}$	M0 [a]/ $M^{-1}cm^{-1}$	C_1 (full abs.) [b]/$M^{-1}cm^{-1}$	C_2 (full abs.) [b]/$M^{-1}cm^{-1}$	C_1 (CD) [c]/deg $M^{-1}cm^{-1}$	C_2 (CD) [c]/deg $M^{-1}cm^{-1}$	C_2 (CD-DeVoe) [d]/deg $M^{-1}cm^{-1}$
340	928 (703)	−2284 (755)	2734	3662	451			
350	−203 (150)	−3808 (638)	3500	3297	−308	−25.4 (4.1)	−14.8 (6.2)	−66
360	−2248 (851)	−5068 (558)	5010	2761	−50	−82.9 (3.5)	−68.7 (6.4)	−94.4
370	−4757 (991)	−5758 (601)	7125	2367	1367	−154.5 (3.8)	−152.5 (5.5)	−145.2
380	−7307 (1110)	−5470 (623)	9689	2381	4219	−236.8 (5.0)	−288.0 (5.3)	−204.4
390	−8470 (1135)	−3325 (623)	12554	4084	9229	−309.1 (4.0)	−428.5 (5.9)	−264
400	−8085 (1096)	−619 (355)	15371	7286	14752	−334.7 (4.6)	−560 (6.6)	−426
410	−8660 (1235)	2780 (401)	17907	9247	20687	−295.5 (3.3)	−628.4 (6.7)	−541
420	−7418 (1176)	4163 (430)	20125	12707	24288	−240.8 (3.1)	−520.5 (6.8)	−527.6
430	−3479 (440)	2995 (410)	22105	18626	25100	−201.8 (4.4)	−245.7 (6.9)	−185
440	1646 (386)	−44 (398)	23907	25553	23863	−200.1 (4.9)	74.6 (6.6)	224
450	8145 (443)	−3418 (507)	25506	33650	22088	−234.5 (5.7)	326.4 (6.7)	384
460	14690 (552)	−6244 (523)	26525	41215	20281	−295.4 (6.1)	462.6 (6.8)	540.8
470	21524 (587)	−8656 (565)	26381	47905	17725	−343.1 (7.6)	442.2 (6.5)	461.6
480	25272 (611)	−9503 (571)	24756	50028	15253	−366.8 (6.0)	390.9 (6.3)	342.8
490	26405 (662)	−9402 (570)	21699	48100	12297	−368.7 (6.2)	323.3 (6.1)	251
500	23400 (735)	−8890 (563)	17609	41009	8719	−320.2 (6.2)	278.5 (5.2)	184.8
510	16754 (500)	−7999 (551)	13090	29844	5090	−248.4 (5.6)	245.5 (5.1)	145.2
520	9559 (471)	−6552 (544)	8865	16424	2313	−153.5 (4.6)	201.9 (5.4)	105.6
530	3556 (401)	−4611 (532)	5426	8982	815	−83.1 (4.4)	154.2 (6.4)	85.6
540	1437 (386)	−2987 (529)	2993	4429	150	−33.0 (3.6)	81.8 (6.6)	66
550	959 (312)	−1713 (499)		2500	30			
560	901 (299)	−716 (460)		1500	15			

[a] Molar absorptivities of Methyl Orange taken from a 3×10^{-5} M solution of the dye in the same buffer (pH = 7.0). [b] Calculated from the algebraic sum of the computed difference absorbance values and corresponding absorptivities of the free dye. [c] The reported standard deviations in parentheses represent the results of the fitting; these values can be less relevant than deviations due to experimental errors. [d] CD values obtained through the application of the DeVoe method to the C_2 complex considered as an unique chromophore (see Results).

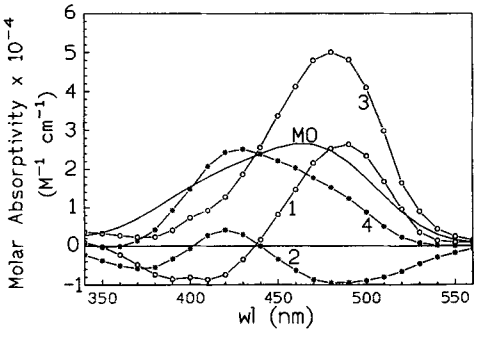

Fig. 3. Fitted difference molar absorptivties for C_1 (curve 1) and C_2 (curve 2), and full molar absorptivities for C_1 (curve 3) and C_2 (curve 4), compared with the MO curve in the 340–560 nm interval.

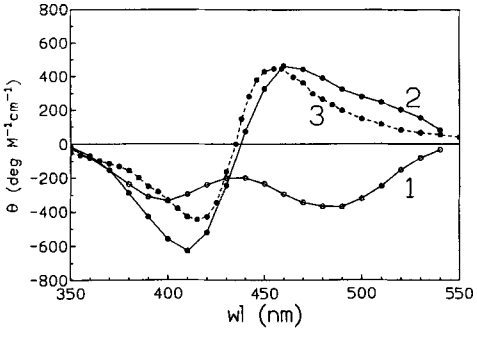

Fig. 4. Fitted CD spectra of C_1 (curve 1), C_2 (curve 2), and calculated dichroic spectrum for C_2 complex according to the DeVoe method (curve 3).

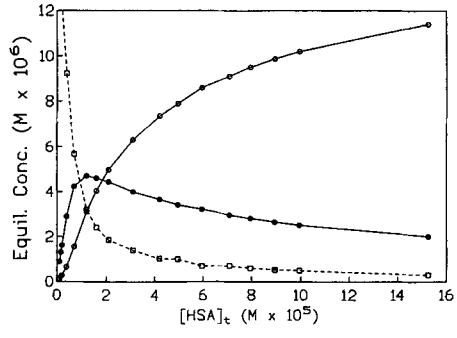

Fig. 5. Equilibrium concentrations of C_1 (○), C_2 (●), and $[MO]_{free}$ (□) calculated on the basis of the fitted $K_{1,1}$ and $K_{1,2}$ association constants for $[MO]_t = 1.57 \times 10^{-5}$ M and $[HSA]_t = 0.102-15.26 \times 10^{-5}$ M.

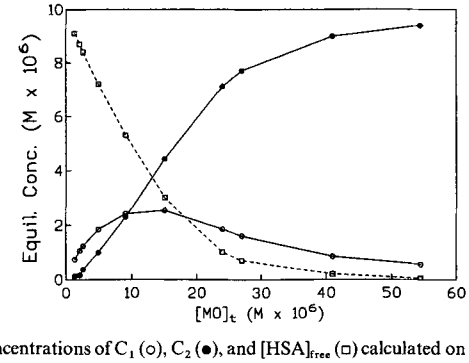

Fig. 6. Equilibrium concentrations of C_1 (○), C_2 (●), and $[HSA]_{free}$ (□) calculated on the basis of the fitted $K_{1,1}$ and $K_{1,2}$ association constants for $[HSA]_t = 0.9 \times 10^{-5}$ M and $[MO]_t = 0.13-5.44 \times 10^{-5}$ M.

ciple be reached through well-known, traditional methods. Of these, the Scatchard equation is the mostly widely used,[12] because it allows the number of effective *equivalent* binding sites and the values of the association constants of the complexes to be calculated from a single plot. In the form reported as Equation (9), the association constant K is obtained directly as the

$$\nu/L = nK - \nu K \quad (9)$$

0947-6539/96/0202-0152 $ 10.00+.25/0 Chem. Eur. J. 1996, 2, No. 2

slope of the straight line resulting from the plot of v/L versus v, while the number of binding sites n is obtained from the intercept on the v axis. The term v is defined as the number of molecules of the ligand bound per molecule of the protein, and L represents the concentration of free ligand.

We applied the Scatchard procedure to the data of the difference absorbances registered at 490 nm as a function of the analytical concentrations of HSA. At a fixed MO concentration of 1.57×10^{-5} M, a saturation of the ligand at the highest concentrations of protein ($10-15 \times 10^{-5}$ M) seems to take place (Fig. 1, curves 1). Under the assumption that only the 1:1 complex was present at these concentrations, a molar absorptivity ε of 17000 $cm^{-1}M^{-1}$ can be evaluated for C_1. On the basis of this value, the amount of both bound and free ligands and also the term v can be calculated, and the unfilled circles of Figure 7 are obtained. These scattered points resemble a sigmoid; the intercept on the y axis of a hypothetical straight line going through the majority of them is around 1.4×10^5, not too different from the computed value for $K_{1,1}$ of $2.23 \times 10^5\ M^{-1}$, and the intercept on the v axis gives the unacceptable value of 0.7 (number of equivalent binding sites).

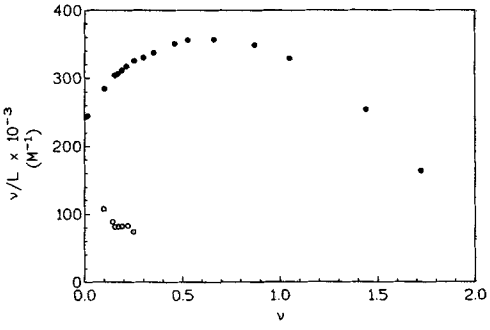

Fig. 7. Scatchard plots of the bound fraction calculated on the basis of a limiting $\varepsilon_{490} = 17000\ M^{-1}cm^{-1}$ for C_1 complex (o) and through the equilibrium concentrations of both C_1 and C_2 complexes, calculated using the fitted $K_{1,1}$ and $K_{1,2}$ association constants (•).

A completely different but interesting plot is obtained by calculating the equilibrium concentrations of all species on the basis of the two fitted values $K_1 = 2.325 \times 10^5\ M^{-1}$ and $K_2 = 4.83 \times 10^5\ M^{-1}$, at the same analytical MO concentration of 1.57×10^{-5} M, while the concentration of HSA is allowed to vary between 1×10^{-3} and 1×10^{-6} M. The resulting Scatchard plot is shown in Figure 7 (filled circles). The concave appearance of the plot is considered a sufficient criterion for positive cooperativity: in this case the intercept with the y axis gives an estimate of K_1; the slope at high v values gives $-nK_1$, while the initial slope equals $2K_2 - K_1$.[16] Moreover, an estimate of the Hill coefficient n_H can be obtained from the value of v at the maximum of Scatchard plot, according to Equation (10).

$$n_H = v/(n - v) \tag{10}$$

On the basis of the intercept of the curve with the v/L axis ($\approx$240000), the slope at the highest v values ($\approx -$ 231000), the initial slope ($\approx$435000), and the v value at the maximum of the Scatchard plot ($\approx$0.6), the following set of binding parameters can be evaluated: $K_1 = 240000\ M^{-1}$, $n = 1$, $K_2 = 340000\ M^{-1}$, and $n_H = 1.5$. An acceptable match is obtained between the values of the two formation constants and those obtained through the fitting procedure.

Ultrafiltration: In order to directly verify the extent of MO complexation by HSA, an aqueous buffered solution (pH = 7) of MO and HSA in a molar ratio [MO]/[HSA] = 5.8 was subjected to ultrafiltration. The percentage of free MO in the solution was 67%. On average, up to two molecules of MO were complexed to each HSA, as found in the fitting procedure.

Calculation of the CD Spectrum of the C_2 species (DeVoe Method): As shown above, C_1 and C_2 complexes are endowed with CD properties (see Fig. 3 and 4), which provide specific information on the geometry of the C_2 complex. When dealing with an aggregate of molecules, an independent-system approach, such as the DeVoe treatment,[17] seems particularly suited to the calculation of chiroptical properties. According to the DeVoe method the "independent systems" are the chromophores; here, they are really "independent" of each other, since they are localized on different MO molecules. These subsystems are polarized by the external electromagnetic radiation and are coupled to each other by their own dipolar oscillating fields. Within the framework of classical physics, the optical properties (absorption, refraction, optical rotatory dispersion, and circular dichroism) of the aggregate of subsystems are calculated, taking into account, in addition to the above interactions, the polarizability of the chromophore, an exclusively quantum mechanical quantity. The imaginary part of the complex polarizability can be obtained directly from the absorption bands of the chromophore and the real part by means of its Kronig–Kramers transform. As far as the direction of the polarization of the chromophore transition is concerned, general information as well as symmetry considerations on the MO molecule point to a direction along the long molecular axis. Thus, the problem has been reduced to calculating the optical consequences of the coupling of two oscillating equal dipoles, which are almost parallel and separated by about 10 Å. The polarizability of the dipoles was deduced from the measured absorption spectrum of a monomeric MO, and the interchromophoric distance $R_{1,2}$ was derived from simple molecular modeling. The dissymmetry necessary to obtain an optically active system is dependent on the angle of rotation ϕ of the second dipole P_2 around the interdipole axis $R_{1,2}$: a non-zero ϕ angle is required in order to avoid zero CD. This angle ϕ was considered to be a variable parameter in order to fit the experimental CD couplet attributed to the C_2 complex, while the MO absorption corresponding to the band centered at 435 nm was described by means of a Gaussian band with a dipolar strength μ^2 of 28 D^2 with a $3.7 \times 10^3\ cm^{-1}$ bandwidth. In agreement with the very small ϕ angle of 0.7°, we obtain a CD curve that overlaps satisfactorily with that obtained from the fitting procedure for the same C_2 complex, shown as curve 3 in Fig. 4 (dashed line); the relative calculated data are reported in Table 2. It should be noted that an equally valid fitting of the CD spectrum of C_2 complex can also be obtained at a different interchromophoric distance $R_{1,2}$, corresponding to different ϕ values. For example, with $R_{1,2} = 5$ Å, the value of $\phi = 0.18°$ practically reproduces curve 3 in Figure 4. In other words, the tighter the dimer, the smaller is the average rotation angle required. In parallel to the CD spectrum, the UV/Vis absorption spectrum, too, is perfectly fitted by DeVoe computations.

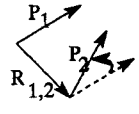

Solvent Effects on Absorbance Spectra of C_1 and C_2 Complexes: Qualitative information on the nature of the noncovalent bonding between the dye and the protein both in C_1 and C_2 can be obtained by comparison of their respective difference ab-

sorbance spectra with the corresponding spectra recorded after adding organic solvents or salts to the aqueous solutions. The spectral changes induced by salts, organic solvents, and polypeptides in Cibacron Blue F3GA dye have been used to ascertain the interactions of the so-called "Blue Dye" with proteins.[18] Similar effects of the microenvironment have also been examined by the absorption changes in Methyl Orange.[19]

A similar approach was applied to the present case. Figure 8 shows the difference absorbance spectra of a 1.5×10^{-5} M Methyl Orange solution in phosphate buffer (pH = 7.0) with various additives: 1.0 M NaCl (curve 1), 50% ethylene glycol (curve 2), 3.8×10^{-6} M HSA with 1.0 M NaCl (curve 3), 4.2×10^{-4} M HSA with 1.0 M NaCl (curve 4), and 4.2×10^{-4} M HSA with 50% ethylene glycol (curve 5).

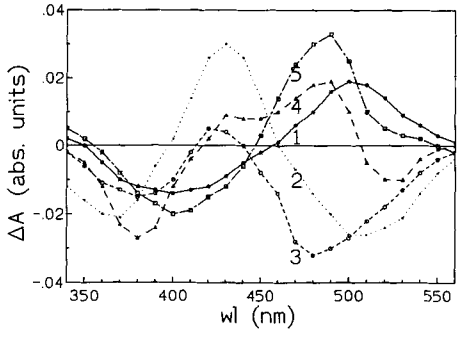

Fig. 8. Difference absorbance spectra of solutions containing [MO] $= 1.5\times10^{-5}$ M in 0.1 M phosphate buffer (pH = 7.0, 1 cm path) with various additives: 1.0 M NaCl (curve 1), 50% ethylene glycol (curve 2), 3.8×10^{-6} M HSA and 1.0 M NaCl (curve 3), 4.2×10^{-4} M HSA and 1.0 M NaCl (curve 4), and 4.2×10^{-4} M HSA and 50% ethylene glycol (curve 5).

It is worth stressing that curves 1 and 5 display approximately the same trends as were observed for the C_1 complex (Fig. 3, curve 1): a positive maximum at 480–500 nm and a negative peak around 400 nm. On the other hand, a similarity with the absorbance spectrum of the C_2 complex is evident in curves 2 and 3, where two negative maxima at 370–380 and 480–500 nm are observed, together with a positive maximum at around 420–430 nm. Curve 4 resembles neither the fitted spectrum of C_1 nor that of C_2.

Since the effects observed could be due to changes occurring to the secondary structure of the protein, control experiments were carried out by recording the CD spectra of 4.2×10^{-5} M albumin dissolved in the reference buffered solution with 50% ethylene glycol or 1.4 M NaCl as additives. In both cases, the dichroic spectra overlapped almost perfectly with the reference recorded in the 250–200 nm range for HSA in buffer.

Discussion

The results show the suitability of the physical model applied to the investigation of the complexation between HSA and MO, which involves two rapid reversible equilibria.

The present approach exhibits some decisive advantages. First, the results of different experimental techniques can be included in the fitting procedure. Although the inclusion of multiwavelength data from both absorbance and CD measurements in an overall fitting results in a multitude of fitting parameters, it is the only available method of circumventing the problems of underdetermination[20] encountered in the study of multiple equilibria. The price is an increase in computational time, but both stability constants and molar spectra for the each complex can be obtained from a single fit.

A further advantage of our approach relates to the conditions used to investigate these complex equilibria. With traditional methodologies, extreme concentrations are required in order to force equilibria towards complete complexation; this allows limiting molar absorptivies or ellipticities to be obtained, needed for the calculation of the bound and free ligand concentrations. In our approach, we can work with data obtained at partial complexation, that is, under average, standard conditions. Moreover, in the system under investigation, we can go as far as to say that no saturation spectrum can ever exist for the 1:1 species. Figure 5 makes it clear that there is no experimentally accessible concentration at which it is possible to force full formation (with respect to the deficient reagent) of the 1:1 complex without causing appreciable formation of the 1:2 complex. Thus, the saturation shown in Figure 1 is only apparent and is due to partial compensation from the disappearance C_2 ($\varepsilon_{490} = -9402\,M^{-1}cm^{-1}$, Table 2) and formation of C_1 ($\varepsilon_{490} = 26405\,M^{-1}cm^{-1}$). This is a source of unavoidable error in saturation plots of any type.

Among the outcomes of the fitting procedure, the final root mean square deviation, reported in run 4 of Table 1 (0.087 absorbance or ellipticity units), allows a direct evaluation of the accuracy of the final fitting. Considerable matching of the computed and experimental difference absorbance and dichroic curves is displayed in Figures 1 and 2, too. Moreover, the computed $K_{1,1}$ and $K_{1,2}$ stability constants, and all molar absorptivities and ellipticities are well defined, as shown by their standard deviations, never exceeding 15% of the value of the reference parameter. The correlation coefficient between $K_{1,1}$ and $K_{1,2}$ (0.983, run 4, Table 1), is high, in spite of the large number of experimental points (879) included in the fitting procedure and of the wide concentration range of both protein and dye examined in the spectrophotometric experiments. However, the fact that the number differs significantly from 1 indicates that the $K_{1,1}$ and $K_{1,2}$ values, even if correlated, maintain individual significance.

Cooperativity: In the present case, the C_2 complex is present in significant concentrations over the full range of experimentally attainable HSA concentrations, as shown in Figures 5 and 6. Neither the assumption that the second equilibrium [Eq. (5)] is negligible nor the inference of the molar extinction coefficient based on the apparent saturation of the first complex are therefore correct. We conclude that, if positive cooperativity does occur, it is extremely difficult, or even impossible, to obtain a correct Scatchard plot on the basis of more or less reliable assumption of ligand saturation. By extension, a similar conclusion could also affect the application of the Edsall method,[21] the Bjerrum plot,[22] or the Klotz equation,[1d] all of which are based upon the assumption of a limiting molar absorptivity, ellipticity, or fluorescence intensity[23] of the investigated complex(es). Only after the "true" bound ligand has been evaluated, taking into account the equilibrium concentrations of both complexes, obtained from the fitted parameters, does the Scatchard plot show the expected trend (Fig. 7). This "corrected" plot gives unique information: 1) the number of the equivalent binding sites $n = 1$, which allows us to conclude that the second molecule of Methyl Orange fits into the same site as for the C_1 complex and that the C_2 complex therefore actually contains two molecules of ligand bound in a single site; and 2) the Hill coefficient $n_H = 1.5$, indicative of cooperative binding.[24] A similar conclusion can be also inferred on the basis of $2K_2 - K_1 > 0$.[17]

0947-6539/96/0202-0154 $ 10.00+.25/0 Chem. Eur. J. 1996, 2, No. 2

The occurrence of positive cooperativity can be deduced by careful inspection of Figure 5, where the consequences of the very high association constants for C_1 and C_2 complexes ($K_1 = 2.32 \times 10^5\,M^{-1}$ and $K_2 = 4.83 \times 10^5\,M^{-1}$) appear evident. As expected, the equilibrium concentrations of C_1 increases as the total albumin concentration increases. At the highest $[HSA]_t = 1.53 \times 10^{-4}$ M, Methyl Orange is still not completely complexed as the C_1 species. The latter only starts to prevail over C_2 at $[HSA]_t \geq 2 \times 10^{-5}$ M, but, even then, C_2 still makes a contribution to the overall complexation of the dye of 18% (36% when the 2:1 dye/protein stoichiometry in this complex is considered). The determination of the limiting spectra of C_2 suffers from a similar uncertainty. At the highest dye concentration, the $[C_1]_{eq}$ contribution to the saturation of HSA is not negligible, even in though C_2 is present in much higher concentrations (Fig. 6). In cases where overlapping protein–ligand equilibria all contribute to the overall measured physical quantity and only one complex is taken into account, we expect a failure of traditional data-handling methodologies.

Interactions in HSA–MO Complexes: It is well known that protein–ligand interactions comprise a wide range of noncovalent forces, ranging from hydrogen bonding and electrostatic effects to charge-transfer complexation, π stacking, and hydrophobic effects.[25] Since two different complexes between HSA and MO were spectroscopically characterized, it was of interest to investigate the interactions that allow their formation and to confirm that the 1:2 C_2 species contains two MO units in the same binding site of the protein.

Significant, even though indirect, information is provided by careful inspection of the UV/Vis absorbance spectra of both C_1 and C_2 species, and by the spectral changes occurring in the absorption spectrum of MO in the presence of either ethylene glycol or NaCl, both with and without added HSA. The influence of complexation with the protein on the electronic spectrum of Methyl Orange can be better understood by comparing the full spectrum of C_1 and C_2 with that of the free dye. In Figure 3 we report the full UV/Vis spectra of both C_1 (curve 3) and C_2 (curve 4) complexes, together with that of MO.

The spectral changes occurring when bovine or human serum albumin are added to aqueous solutions of Methyl Orange have been known for a long time and have been attributed to strong electrostatic dye–protein interactions between specific, protonated amino groups of the protein and the sulfonate group of MO.[3a, 26, 27] Similar shifts of the absorption band of the azo dye were found to take place on changing solvents.[26] Upon addition of excess HSA, bathochromic and hyperchromic shifts of the visible absorption band of MO were found in buffered solution, while progressive hypsochromic and hypochromic displacements were observed with increasingly apolar solvents. The latter type of effect is also observed upon addition of small amounts of HSA, and has been attributed to the steric strain in the dye induced on complexation to the albumin or to the decrease in a specific interaction (hydrogen bonding) with the aqueous solvent.[10]

Although the above discussed effects had been attributed to a generic complexation of MO with bovine or human serum albumin, on the basis of the fitting results we can reasonably attribute to C_1 the first-discussed spectral changes, while the second type can be ascribed to the presence of C_2. Dye–dye interactions and steric constraints can easily be envisaged to explain the accommodation of two MO units into the same binding site. The fact that the latter effect is thought to predominate in most cases can be attributed to the positive cooperativity found for the formation of the C_2 complex, discussed above.

Further information concerning the nature of the protein–dye interactions can be derived from the spectral evidence reported in Figure 8. Comparison with the two UV/Vis difference spectra in Figure 3 reveals that electrostatic interactions predominate in the C_1 complex, while hydrophobic forces prevail in the C_2 complex. In the presence of both HSA (3.8×10^{-6} M) and NaCl (1.0 M), the difference spectrum of MO changes from curve 1 to curve 3, which is similar to the C_2 fitted spectrum. On addition of HSA to MO dissolved in a 50% ethylene glycol/buffer mixture, a drastic change occurs at $[HSA]_t = 4.8 \times 10^{-4}$ M from curve 2 to 5, which is very similar to the fitted spectrum of the C_1 complex. Curve 4 was recorded under the same conditions as curve 3, but at much higher $[HSA]_t = 4.2 \times 10^{-4}$ M. It represents an intermediate situation, in which both complexes are apparently contributing to the absorbance. Finally, control measurements on HSA solutions, in the presence of 1.4 M NaCl or 50% ethylene glycol, gave identical spectra in the 350–200 nm interval, and overlapped the reference CD spectrum of HSA. We conclude that the addition of NaCl or ethylene glycol does not change the secondary structure of the protein. Thus, electrostatic interactions appear to predominate between dye and protein in the C_1 complex and hydrophobic interactions in the C_2 complex. A stacking process can be envisaged to take place in the C_2 complex, as discussed below. The protonated amino group could interact with the sulfonic moiety of each MO unit; this would allow the aggregation between the two whole chromophores.

Chirality: An induced dichroism arising from dimeric MO units bound to poly-L-lysine (PLL) has been used to show an (*S*) chirality of these dye molecules, considered as two chromophores bound through their sulfonate groups to the same protonated amino residue.[5c] This interpretation, incorporating a strong stacking interaction between the two bound MO molecules, was later enriched to include different bound states of MO attached to the PLL polymer. Interestingly, at low protein/dye ratios, an almost parallel stacking ($\alpha \approx 0°$) was envisaged for closely bound MO molecules.[28]

A similar interpretation can be invoked here, because of the appearance of an exciton couplet in the CD-fitted spectrum of C_2 species. This finding allows us to reasonably consider the two dye units as a unique bichromophoric molecule, endowed with a (*R*) chirality (Fig. 9).[29] This interpretation is supported by

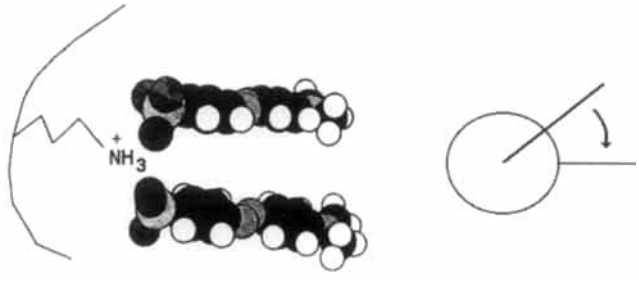

Fig. 9. Schematic geometry for the C_2 complex and (*R*) chirality of the dipole transition moments of MO.

the CD spectrum of the same C_2 species calculated according to the DeVoe method (Fig. 4, curve 3) assuming a 5–10 Å separation between the stacked MO units and a 0.2–0.7° angle between molecular axes. The almost perfect overlap of the fitted and calculated CD spectra points to a unique binding site for the two MO unities, and can be considered as decisive support for the entire concept of HSA–MO complexation.

Experimental Section

Materials: Human Serum Albumin (HSA) A-1653 Frac. V was purchased from Sigma (96-99%), stored at 4°C, and used without further purification. At the highest concentrations, HSA exhibited a weak absorption band centered at 405 nm, devoid of any CD activity and attributable to an impurity that could not be identified as a fatty acid or as bilirubin (according to control experiments). In control experiments, CD spectra of HSA were recorded, which exhibited the usual negative dichroic absorption in the 350-200 nm range. Methyl orange (MO, sodium 4-dimethylaminoazobenzene-4-sulfonate) was purchased from C. Erba (TLC, pure).

Spectrophotometric Measurements: HSA and MO were dissolved in the selected concentration ranges in buffered (pH = 7.0) water solutions, prepared by adding 0.1 N NaOH to a solution of 0.1 M NaH_2PO_4 up to the required pH value. UV/Vis spectra were recorded on a Perkin-Elmer Lambda 2S instrument, with 1 nm bandwidth and a 1 cm cell thermostatted at 25°C, by using the so-called "difference absorbance technique" [11]. This technique allows the small differences in absorption induced by complexation of the dye with albumin in the sample cell, with respect to a reference solution containing an identical dye concentration in the same buffered water solution, to be read directly.

CD spectra were registered on a Jasco J-600 spectropolarimeter, with a 2 nm bandwidth and a 5 cm cell thermostatted at 25°C. J-600 PC software was used to record CD spectra. The reference solution consisted of a cell containing only the buffer. Control experiments showed that no dichroic activity was exhibited by albumin in the 350-550 nm interval.

The spectrophotometric data are the results of at least three independent, perfectly reproducible measurements. Many CD and difference absorbance measurements were also checked by preparing solutions containing the same analytical concentrations of HSA and MO by different procedures. The usual method consisted in the preparation of stock solutions containing the highest reported concentration of the excess species (either HSA or MO) and appropriate concentrations of the other material (MO or HSA, respectively). These stock solutions were then diluted with appropriate volumes of a solution containing the species at the concentration chosen to be constant during the measurements. In addition to this method, the following dilution techniques were also used: a) preparation of both HSA and MO stock solutions, which were then mixed in the selected ratios; b) preparation of a stock solution containing both HSA and MO, which was then diluted with suitable volumes of the buffer; and c) preparation of a stock MO solution, to which appropriate amounts of weighed albumin was directly added. In all cases both the CD and UV/Vis spectra agreed independently of the method used to obtain the given concentrations of HSA and MO.

Fitting Procedures: The overall data set consists of slightly less than 1000 vectors, each consisting of five experimental data points (two concentrations, wavelength, optical path, absorbance, and ellipticity). Ellipticities were associated with "dummy" wavelength values, obtained from the true ones by adding 300 nm. This simple trick eliminated possible ambiguities from absorbances and ellipticities measured at the same wavelength. The number of fitting parameters was also large, including the two formation constants together with a number of molar absorbances and ellipticities. This meant that a workstation (IBM R6000/580) with a large memory was required to perform calculations with a FORTRAN program. Fitting took a few seconds on the workstation. The small contribution from the impurity present in albumin to measured difference spectra was taken into account by adjusting the molar absorptivities of albumin itself in the short wavelength range where this unwanted absorption was apparent.

Ultrafiltration Experiments: A buffered solution (pH = 7) containing [HSA] = 1×10^{-5} M and [MO] = 5.8×10^{-5} M was filtered through a Spectrum CK 20 membrane. The concentration of free dye was deduced from UV/Vis spectrum of the filtrate.

CD "DeVoe" Calculations: A FORTRAN program was used to calculate the polarizability values corresponding to the absorption band attributed to each MO moiety at frequencies between 18000 cm^{-1} (555.5 nm) and 29000 cm^{-1} (344.8 nm); a step size of 200 cm^{-1} was used. Then, the appropriate DeVoe equations [17], in which coupling terms depended on the assumed geometry of the MO units, were resolved by the same program at each frequency. This process finally yielded the UV, CD, and ORD data for comparison with experimental results.

Acknowledgements: This work was supported from MURST and CNR.

Received: June 7, 1995 [F145]

[1] a) K. Murakami, *Bull. Chem. Soc. Jpn.* **1988**, *61*, 1323; b) F. Karush, *J. Am. Chem. Soc.* **1951**, *73*, 1246; c) F. Karush, *ibid.* **1950**, *72*, 2705; d) I. M. Klotz, F. M. Walker, R. B. Pivan, *ibid.* **1946**, *68*, 1486.

[2] X. M. He, D. C. Carter, *Nature* **1992**, *358*, 209.

[3] a) I. M. Klotz, *J. Am. Chem. Soc.* **1968**, *68*, 2299; b) I. M. Klotz, R. K. Burkhard, J. M. Urquhart, *J. Phys. Chem.* **1952**, *56*, 77; c) I. M. Klotz, R. K. Burkhard, J. M. Urquhart, *J. Am. Chem. Soc.* **1952**, *74*, 202.

[4] See for instance: M. T. Beck, I. Nagypal in *Chemistry of Complex Equilibria* (Ed.: D. R. Williams), Ellis Horwood, **1990**. See also: G. Dodin, J. Aubard, D. Falque, *J. Phys. Chem.* **1987**, *91*, 1166.

[5] a) I. S. Cho, T. Komoto, T. Kawai, *Macromol. Chem.* **1980**, *181*, 193; b) T. Takagishi, N. Kuroki, *J. Polym. Sci. Polym. Chem. Ed.* **1973**, *11*, 1889; c) M. Hatano, M. Yoneyama, Y. Sato, Y. Kawamura, *Biopolymers* **1973**, *12*, 2423; d) F. Quadrifoglio, V. Crescenzi, *J. Coll. Int. Sci.* **1971**, *35*, 447; e) I. M. Klotz, G. P. Royer, A. R. Sloniewsky, *Biochemistry* **1969**, *8*, 4752; f) L. Styrer, E. R. Blout, *J. Am. Chem. Soc.* **1961**, *83*, 1411; g) E. R. Blout, L. Styrer, *Proc. Natl. Acad. Sci. USA* **1959**, *45*, 1591.

[6] S. B. McLoughlin, C. R. Lowe, *Rev. Prog. Color. Rel. Top.* **1988**, *18*, 16, and references therein.

[7] a) Y. Kroviarski, S. Cocchet, S. Vador, P. Truskolaski, P. Bovin, O. Bertrand, *J. Chromatogr.* **1988**, *449*, 403; b) E. Miribell, E. Gianazzo, P. Arnaud, *J. Biochem. Biophys. Methods* **1988**, *16*, 1; c) S. J. Burton, S. B. McLoughlin, C. V. Stead, C. R. Lowe, *J. Chromatogr.* **1988**,*435*, 127; d) R. K. Scopes, *Anal. Biochem.* **1987**, *104*, 235; e) C. R. Lowe, S. J. Burton, Y. D. Clonis, J. C. Pearson, *J. Chromatogr.* **1986**, *376*, 121.

[8] a) S. J. Burton, C. R. Lowe, C. V. Stead, *J. Chromatogr.* **1986**, *455*, 201; b) J. P. Pearson, S. J. Burton, C. R. Lowe, *Anal. Biochem.* **1986**, *158*, 383; c) C. R. Lowe, S. J. Burton, J. C. Pearson, Y. D. Clonis, C. V. Stead, *J. Chromatogr.* **1986**, 376, 12.

[9] a) K. M. Tawarash, A. A. Wazwaz, *Ber. Bunsenges. Phys. Chem.* **1993**, *97*, 727; b) S. K. Lee, W. S. Kim, *Polymer* **1993**, *34*, 2392; c) K. Murakami, T. Sano, N. Kure, K. Ishii, T. Yasunaga, *Biopolymers* **1983**, *22*, 2035; d) C. E. Williamson, A. H. Corwin, *J. Colloid. Interfac. Sci.* **1972**, *38*, 577; e) I. M. Klotz, *J. Am. Chem. Soc.* **1968**, *68*, 2299; f) G. Marcus, *Proc. Natl. Acad. Sci. USA* **1965**, *54*, 253; g) E. Prokopova, P. Munk, *Collect. Czech. Chem. Commun.* **1963**, *28*, 957; h) L. A. E. Ashworth, C. Green, *Biochem. Biophys. Acta* **1963**, *70*, 68; i) G. Oster, *J. Polym. Sci.* **1955**, *16*, 235; j) G. Oster, *ibid.* **1952**, *9*, 553; k) I. M. Klotz, R. K. Burkhard, J. M. Urquhart, *J. Am. Chem. Soc.* **1952**, *74*, 202; l) F. Karush, *ibid.* **1951**, *73*, 1246; m) I. M. Klotz, F. M. Walker, R. B. Pivan, *ibid.* **1946**, *68*, 1486.

[10] R. L. Reeves, R. S. Kaiser, M. S. Maggio, E. A. Sylvestre, W. H. Lawton, *Can. J. Chem.* **1973**, *51*, 628.

[11] C. R. Cantor, P. R. Schimmel, *Biophysical Chemistry*, W. H. Freeman, New York, **1980**, Part II, Chapter 7.

[12] a) G. Scatchard, J. S. Coleman, A. L. Shen, *J. Am. Chem. Soc.* **1957**, *79*, 12; b) G. Scatchard, *Ann. N. Y. Acad. Sci.* **1949**, *51*, 660.

[13] G. Bellucci, R. Bianchini, C. Chiappe, F. Marioni, R. Ambrosetti, R. S. Brown, H. Slebocka-Tilk, *J. Am. Chem. Soc.* **1989**, *111*, 2640.

[14] a) W. C. Hamilton, *Statistics in Physical Science*, Ronald, New York, **1995**; b) Y. Bard, *Non-Linear Parameter Estimation*, Academic Press, New York, **1974**.

[15] I. S. Berezin, N. P. Zhidkov, *Computing Methods*, Pergamon, Oxford, **1965**, Vol II, p. 136.

[16] B. Perlmutter-Hayman, *Acc. Chem. Res.* **1986**, *19*, 90.

[17] a) M. Zandomeneghi, C. Rosini, P. Salvadori, *Chem. Phys. Lett.* **1976**, *44*, 533; b) H. DeVoe, *J. Chem. Phys.* **1964**, *41*, 393; *ibid.* **1965**, *45*, 3199.

[18] S. Subramanian, *Arch. Biochem. Biophys.* **1982**, *216*, 116.

[19] K. I. Papathomas, S. C. Israel, J. C. Salamone, *J. Appl. Polym. Sci.* **1989**, *38*, 1077.

[20] R. Brodersen, F. Nielsen, J. C. Christiansen, K. Andersen, *Eur. J. Biochem.* **1987**, *169*, 487.

[21] a) J. H. K. Ma, H. W. Jun, L. A. Luzzi, *J. Pharm. Sci.* **1973**, *62*, 2038; b) J. T. Edsall, C. Felesenfeld, D. S. Goodman, F. R. N. Gurd, *J. Am. Chem. Soc.* **1954**, *76*, 3054.

[22] J. Bjerrum, *Kgl. Dusk. Vidensk. selek. Math. Phys. Med.* **1944**, *21 (4)*, 3.

[23] D. V. Naik, L. Paul, R. M. Threatte, S. G. Schulman, *Anal. Chem.* **1975**, *47*, 267.

[24] C. R. Cantor, P. R. Schimmel, *Biophysical Chemistry*, W. H. Freeman, New York, **1980**, Part III, Chapter 15.

[25] See, for instance: Y. Li, Y. Hsieh, J. D. Henion, T. D. Ocain, G. A. Schieheser, B. Ganem, *J. Am. Chem. Soc.* **1994**, *116*, 7487, and references therein.

[26] a) W. F. Forbes, B. Milligan, *Austr. J. Chem.* **1962**, *15*, 41; b) W. R. Brode, I. L. Geldin, P. E. Spoerrie, G. M. Wyman, *J. Am. Chem. Soc.* **1955**, *77*, 2762.

[27] a) R. L. Reeves, *J. Am. Chem. Soc.* **1966**, *88*, 2240; b) R. L. Reeves, W. F. Smith, *ibid.* **1963**, *85*, 724; c) H. H. Jaffe, S. Yeh, R. V. Gardner, *J. Mol. Spectrosc.* **1958**, *2*, 120.

[28] K. Murakami, S. Takeyuki, N. Kure, K. Ishii, T. Yasunaga, *Biopolymers* **1983**, *22*, 2035.

[29] N. Harada, K. Nakanishi, *Acc. Chem. Res.* **1972**, *5*, 257.

0947-6539/96/0202-0156 $ 10.00+.25/0